Solvent Effects on the Cleavage of Emodin's Non H-bonded O-H Link: A Theoretical Study

ABSTRACT

Although Emodin is a well-known natural antioxidant, not much is documented on how the cleavage of its free O-H bond (non-hydrogen bond donor) is affected by solvation. Herein, we report on a Density Functional Theory (DFT) study of solvent effects on the enthalpy of homolytic and heterolytic cleavage of this bond in the most stable conformer of emodin. This cleavage results in the release of an atom of hydrogen from emodin, whatever the mechanism adopted. The B3LYP functional has been associated with the 6-311++G** basis set in this work while solvent effects have been investigated via the IEF-PCM approach. Our results show that, contrary to available research which indicates that solvation modifies the antioxidant mechanism, emodin's antioxidant mechanism remains unaltered throughout transition from the gas to the solvent phase. This observation is peculiar to emodin among the plethora of known antioxidant molecules. Emodin preferentially exerts its antioxidant effect through the homolytic hydrogen atom transfer mechanism.

Keywords: DFT, solvation, emodin, antioxidant properties, NBO analysis

1. INTRODUCTION

Nowadays, it is well established that free radicals are fully responsible for the aging process and are a major cause of endemic diseases (cancer, diabetes, cardiovascular dysfunction, cataract, atherosclerosis, asthma, arthritis) and neurodegenerative disorders (Alzheimer's, Parkinson's diseases, and dementia). These endemic diseases result from the degradation of cellular constituents such as lipids, proteins and DNA as a consequence of the action of reactive oxygen species among which we find free radicals [1-3]. Free radicals are very unstable but reactive substances having at least a free electron in their orbitals [4]. Their presence in an organism is as a result of metabolic reactions which are indispensible in their proper functions. Oxidative stress is a direct consequence of excesses in free radicals in the system. A major solution to these problems is the use of antioxidant substances. These are substances which in small amounts with respect to the substrate are susceptible to oxidation and therefore have the potential to prevent or to slow down the oxidation of the substrate [5, 6]. They generally react according to the different modes of their acidic hydrogen atom transfer: hydrogen atom transfer (HAT), single-electron transfer followed by proton transfer (SET-PT), and sequential proton loss electron transfer (SPLET) (see scheme 1). They also react through their chelating ability (or oxidation inhibitory effect) towards metallic ions. The stability of the resultant entity depends on hydrogen bonds, resonance and conjugation effects. It is in this perspective that free OH bonds have been the principal focus of this work. It is noteworthy here that the antioxidant under study (emodin) is an antiviral agent of the anthraquinone family which can be isolated from *rumex abissinicus* [7].

Emodin is a well-known natural product capable of many biological activities. It serves as an active ingredient in the manufacture of certain pharmaceuticals and as an additive in the fabrication of certain cosmetics [8, 9]. It is also used as a purgative, antipyretic, antiviral agent, etc. On an industrial level, it plays a role in oxidative degradation of polymers, auto-oxidation of fuels and is responsible for the loss of elasticity of rubber and plastics [7-10]. Many research works have been carried out on emodin given its biological importance. Among these, radical scavenging capacity has been extensively reported. Although recent studies [7,10] showed that emodin has inhibitory potentials for superoxide radicals, the mechanisms involved are not fully understood. Gas phase theoretical studies based on structure-activity relationships (SAR) of emodin which were undertaken [8, 9] to understand its antioxidant properties revealed the most stable conformer that is presented in Fig. 1. This is a justification of our choice on

40 emodin conformer investigated in this research endeavor. By these same studies, the free OH group not
41 involved in H-bond formation was shown to be largely responsible for the antioxidant property of emodin.

42 Despite the volume of theoretical work carried out by researchers on emodin, the hydrogen atom transfer
43 mechanism has not yet been established for this molecule. This hydrogen atom transfer by antioxidants
44 could be achieved via heterolytic fission of the O-H bond or by sequential proton loss-electron transfer
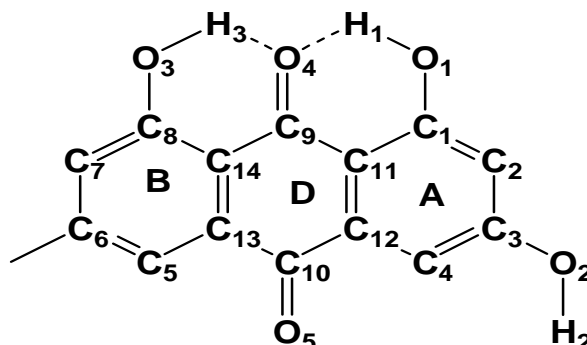45 and single electron transfer-proton transfer reactions as mention above.

46

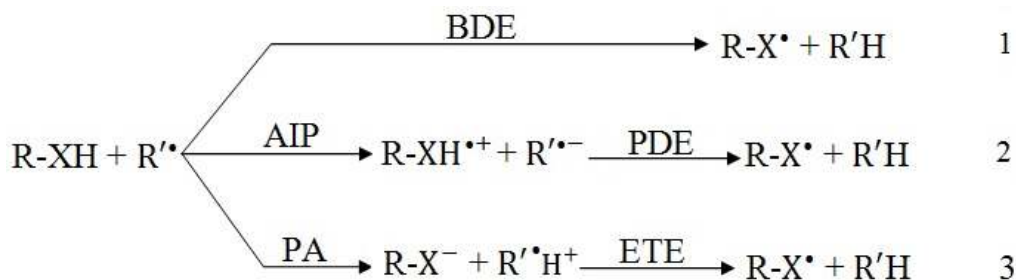47 **Fig. 1. Structure of the most stable conformer of emodin [8, 9]**

48 Because most biological and chemical processes take place in solution, the main focus of this work is on
49 solvent effects. Since solvation can play a critical role on the mechanism of certain processes,
50 examination of solvation's effect on the antioxidant mechanism of emodin is warranted. Investigating
51 solvent effects on the cleavage of the free O-H bond in emodin involves the Bond Dissociation Energy
52 (BDE) studies. The DFT method was chosen for this work because it takes better account of electronic
53 correlation that is necessary for a good estimate of BDE and a good description of the radicalizing
54 species. The DFT/B3LYP level of theory has been used since it gives better BDE results compared to
55 other methods [11, 12]. Solvent effects were studied via the Integral Equation Formalism Polarizable
56 Continuum Model (IEF-PCM) in benzene, methanol, acetonitrile and water. The IEF-PCM is characterized
57 by good, precise and accurate results with less computation efforts required [13-15]. The solvents were
58 chosen based on the increasing order of their dielectric constants from benzene to water.
59
60 **2. COMPUTATIONAL METHODS**
61
62 All quantum chemical calculations have been performed using the Gaussian 09W computational package
63 [16]. The Gaussian 09W software employs the Gaussian-type orbitals in speeding up calculations [17-20].
64 The restricted Kohn-Sham approach has been preferred to unrestricted approach for these calculations in
65 order to minimize spin contamination and to increase precision on energy evaluations [7, 12]. The
66 GaussView 5.0.8 graphical user interface has been used for pre and post processing of molecular data.
67 The molecular geometry of emodin, radicals and ions in each medium, have been optimized using
68 B3LYP/6-311++G(d,p) level of theory without constraints of any kind. Vibrational frequencies have been
69 calculated at the same level of theory as that used for geometry optimization and no imaginary
70 frequencies were found, ascertaining that the optimized structures are minima on their potential energy
71 surfaces. To obtain very precise results, we chose the large Pople-style basis set 6-311++G(d,p). In order
72 to determine partial charges, second order perturbation or interaction energies and orbital occupations,
73 natural bond orbitals (NBO) analyses were performed on each molecule studied. Solvent contributions
74 were accounted for by means of the IEF-PCM method. This method assumes a homogeneous
75 distribution of the solvent on the entire surface of the aqueous solution [21-24].

76 Free radicals can be deactivated in reactions involving antioxidants according to three mechanisms:
77 Hydrogen Atom Transfer (HAT), Sequential Proton Loss Electron Transfer (SPLET) and Single Electron
78 Transfer followed by Proton Transfer (SET-PT) as illustrated in **scheme 1**. Some antioxidant parameters
79 or descriptors related to these antioxidant mechanisms are defined as follows: Bond Dissociation

80 Enthalpy (BDE – for the HAT mechanism), Proton Affinity and Electron Transfer Enthalpy (PA and ETE –
81 for the SPLET mechanism), Adiabatic Ionization Potential and Proton Dissociation Enthalpy (AIP and
82 PDE–for the SET-PT mechanism) [25-28].

$$R\text{-}XH + R'^{\bullet} \begin{cases} \xrightarrow{\quad BDE \quad} R\text{-}X^{\bullet} + R'H & 1 \\ \xrightarrow{\quad AIP \quad} R\text{-}XH^{\bullet+} + R'^{\bullet-} \xrightarrow{\quad PDE \quad} R\text{-}X^{\bullet} + R'H & 2 \\ \xrightarrow{\quad PA \quad} R\text{-}X^{-} + R'^{\bullet}H^{+} \xrightarrow{\quad ETE \quad} R\text{-}X^{\bullet} + R'H & 3 \end{cases}$$

83

84 **Scheme 1: Mechanism of hydrogen atom transfer [25-28]**

85 where R-XH represents an antioxidant, X may be O, C, N or S and R' represents the reactive radicalizing
86 species. The mechanism adopted depends on the reaction medium of the antioxidant [26, 28, 29]. The
87 reaction in **equation 1**, with BDE as the characteristic property, preferentially occurs in the gas phase and
88 in non-polar solvents. In polar solvents, SPLET mechanism (that characterizes **equation 3**) is more
89 appropriate. This process is a form of sequential transfer that begins with the departure of a proton from
90 the antioxidant to the reactive radicalising species, controlled by PA and followed by electron transfer
91 from the proton-deficient antioxidant to the protonic reactive radical; this stage is characterized by ETE.
92 The second form of hydrogen atom heterolytic transfert which starts by electron transfer (characterized
93 by IP) and followed by proton transfer (which is studied by PDE) [6, 30, 31]. Thus, the determination of
94 the afore-mentioned properties will facilitate the follow-up and proper understanding of the mechanisms of
95 hydrogen atom transfer. The antioxidant parameters mentioned above are calculated as described below
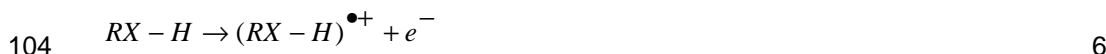96 [32-34]:

97 BDE is a thermodynamic parameter used in characterizing the strength of a chemical bond as shown in
98 equations 4 and 5.

99 $$RX - H \rightarrow RX^{\bullet} + H^{\bullet} \qquad\qquad 4$$

$$BDE = \Delta_f H^{\circ}(RX^{\bullet}) + \Delta_f H^{\circ}(H^{\bullet}) - \Delta_f H^{\circ}(RX-H) \qquad\qquad 5$$

102 where $\Delta_f H^{\circ}(i)$ is the enthalpy of formation of the species i.

103 AIP is the energy necessary to pull out one electron from the antioxidant molecule (equations 6 and 7).

104 $$RX - H \rightarrow (RX - H)^{\bullet+} + e^{-} \qquad\qquad 6$$

105 $$AIP = \Delta_f H^{\circ}((RX - H)^{\bullet+}) + \Delta_f H^{\circ}(e^{-}) - \Delta_f H^{\circ}(RX - H) \qquad\qquad 7$$

106 PDE is the energy responsible for the dissociation a proton from a radical cationic species (equations 8
107 and 9).

108 $$(RX - H)^{\bullet+} \rightarrow RX^{\bullet} + H^{+} \qquad\qquad 8$$

$$PDE = \Delta_f H(RX^\bullet) + \Delta_f H(H^+) - \Delta_f H\left((RX-H)^{\bullet+}\right)$$

109

9

110 PA is the proton dissociation energy of a substance (equations (10 and 11).

$$RX - H \rightarrow RX^- + H^+$$

111

10

$$PA = \Delta_f H°(RX^-) + \Delta_f H°(H^+) - \Delta_f H°(RX-H)$$

112

11

113 ETE is the energy required to remove one electron from an anionic species (equations 12 and 13).

$$RX^- \rightarrow RX^\bullet + e^-$$

114

12

$$ETE = \Delta_f H(RX^\bullet) + \Delta_f H(e^-) - \Delta_f H(RX^-)$$

115

13

116
117
118

3. RESULTS AND DISCUSSION

120

3.1 Solvation effects on geometrical parameters

122

123 The values of selected bond lengths and angles of the most stable conformer of emodin in the various
124 media investigated are presented in **table 1**. Insignificant changes have been observed between the
125 lengths of equivalent C-C bonds in rings A and B in the gas phase; the minimum and maximum
126 discrepancies being 0.001 and 0.008 Å respectively. The C_9-C_{14} and C_9-C_{11} bonds, adjacent to the
127 carbonyl group C_9=O_4 are shorter than the C_{10}-C_{13} and C_{10}-C_{12} bonds by 0.032 and 0.042 Å respectively.
128 These differences can be explained by the fact that the C_9=O_4 group is engaged in the formation of the
129 hydrogen bonds, O_3H_3…O_4 and O_1H_1…O_4. The C_9=O_4 bond being longer than the C_{10}=O_5 bond by 0.042
130 Å, can also be attributed to the involvement of the former in the formation of these hydrogen bonds.
131 Similar observations are made in the case of C_8-O_3 and C_1-O_1 bond lengths, which are each longer than
132 the C_3-O_2 bond.

133 The O_1-H_1 and O_3-H_3 bonds are almost having similar lengths, and are both longer than the O_2-H_2 bond.
134 This is attributable to the involvement of the hydrogen atoms H_1 and H_3 in hydrogen bond formation. The
135 lengths of the hydrogen bonds O_3H_3…O_4 and O_1H_1…O_4 are nearly the same (1.70Å), explaining the
136 similarity in bond lengths between the O_1-H_1 and O_3-H_3 bonds. The angles of these hydrogen bonds are
137 approximately 146°, which is a clear indication that these hydrogen bonds are moderately strong
138 according to the Jeffrey's classification of hydrogen bonds [35].

139 **Table 1. Some lengths (Å) and angles (degrees) of connections of the optimized geometry of the**
140 **most stable conformer of the emodin**

Ring	Bond	Gas	Benzene	Methanol	Acetonitrile	Water
	Bond lengths					
Ring A	C_1-C_2	1.4	1.4	1.4	1.4	1.4
	C_2-C_3	1.39	1.39	1.39	1.39	1.39

	C$_3$-C$_4$	1.4	1.4	1.4	1.41	1.41
	C$_4$-C$_{12}$	1.38	1.38	1.38	1.38	1.38
	C$_1$-C$_{11}$	1.42	1.42	1.42	1.42	1.42
	C$_{11}$-C$_{12}$	1.41	1.42	1.42	1.42	1.42
Ring D	C$_9$-C$_{11}$	1.45	1.45	1.45	1.45	1.45
	C$_9$-C$_{14}$	1.46	1.46	1.46	1.46	1.46
	C$_{10}$-C$_{12}$	1.5	1.5	1.5	1.5	1.5
	C$_{10}$-C$_{13}$	1.49	1.49	1.49	1.49	1.49
Ring B	C$_8$-C$_7$	1.4	1.4	1.4	1.4	1.4
	C$_5$-C$_6$	1.41	1.41	1.41	1.41	1.41
	C$_7$-C$_6$	1.39	1.39	1.39	1.39	1.39
	C$_5$-C$_{13}$	1.38	1.39	1.39	1.39	1.39
	C$_8$-C$_{14}$	1.42	1.41	1.41	1.41	1.41
	C$_{13}$-C$_{14}$	1.42	1.42	1.42	1.42	1.42
	C$_6$-C$_{15}$	1.51	1.51	1.51	1.51	1.51
	C$_1$-O$_1$	1.34	1.34	1.34	1.34	1.34
	C$_3$-O$_2$	1.36	1.36	1.36	1.36	1.36
	C$_8$-O$_3$	1.34	1.34	1.34	1.34	1.34
	C$_9$-O$_4$	1.26	1.26	1.26	1.26	1.26
	C$_{10}$-O$_5$	1.22	1.22	1.22	1.22	1.22
	O$_1$-H$_1$	0.99	0.99	0.99	0.99	0.99
	O$_2$-H$_2$	0.96	0.97	0.97	0.97	0.97
	O$_3$-H$_3$	0.99	0.99	0.99	0.99	0.99
	O$_1$H$_1$…O$_4$	1.7	1.69	1.69	1.69	1.69
	O$_3$H$_3$…O$_4$	1.7	1.69	1.69	1.69	1.69
	Bond angles					
	O$_1$-H$_1$…O$_4$	146.5	146.7	147	147	147

O_3-H_3…O_4	146.1	146.4	146.6	146.7	146.6
C_8-O_3-H_3	107.3	107.2	107.1	107.1	107.1
C_1-O_1-H_1	107.4	107.3	107.1	107.1	107.1
C_3-O_2-H_2	110.1	110.4	110.7	110.8	110.7

141 However, our results have shown that inter-atomic distances remain virtually unchanged from gas to
142 solvent phases. In a general, bond lengths like bond angles almost do not change with solvation. It has
143 been found that hydrogen bond lengths decrease as solvent permittivity increases meanwhile, hydrogen
144 bond angles increase slightly. This predicts that the stability of emodin increases with solvent permittivity,
145 since the decrease in hydrogen bond length increases molecular stability enormously.
146
147 **3.2 Solvent effects on energetic properties**

148 The values of the energetic parameters: thermal energy, E_{therm}, free energy, ΔG°; zero point energy, ZPE,
149 and energy gap, $ΔE_{HOMO-LUMO}$ of emodin in various media are listed in **table 2**. From the values in **Table**
150 **2,** slight reductions in E_{therm}, ΔG and ZPE are observed on going from the gas phase to benzene and from
151 benzene to the polar solvents. The values of these parameters remain nearly the same from one polar
152 solvent (methanol, acetonitrile and water) to another. The greatest reduction in each of these parameters
153 from gas to solvent phases occurs in the case of water; for instance, a maximum reduction of about 33
154 kJ/mol in thermal energy is observed as the gas phase molecule passes into an aqueous medium. Similar
155 reductions of about 36 and 2 kJ/mol for free energy and ZPE respectively are equally observed. This can
156 be explained by the fact that emodin-solvent interactions in non-polar aprotic solvents are Van der Waals
157 in nature, whereas in polar solvents they are hydrogen-bridge in nature (more intense than the former).
158 Thus, at 0 and 298.15 K, the stability of emodin increases slightly with the permittivity of the medium. This
159 trend is similar to the slight increase in hydrogen bond strength with permittivity of the medium as
160 discussed in **section 3.1**.

161 HOMO-LUMO energy gaps are generally used to describe molecular reactivity. It is well established that,
162 the smaller the energy gap, the more reactive is a molecule [36, 37]. The values of emodin's HOMO-
163 LUMO energy gaps are presented in **table 2**. It can be seen that these values remain virtually unchanged
164 from gas to solvent media, which indicates that the global reactivity of this molecule is almost not affected
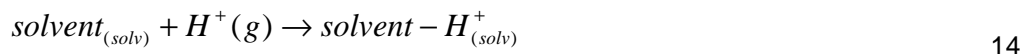165 by solvation.

166 **Table 2. Values of some energetic parameters describing the stability of the emodin, obtained by**
167 **DFT/B3LYP/6-311++G(d,p)**

Parameters	Gas	Benzene ($\varepsilon = 2.28$) [27]	Methanol ($\varepsilon = 32.70$)	Acetonitrile ($\varepsilon = 36.60$) [27]	Water ($\varepsilon = 78.40$) [27]
E_{therm}(kJ/mol)	-2504862	-2504877	-2504894	-2504894	-2504895
$ΔG°$ (kJ/mol)	-2504400	-2504417	-2504436	-2504437	-2504436
ZPE (kJ/mol)	577	576	575	575	575
E_{HOMO} (eV)	-6.75	-6.74	-6.74	-6.74	-6.74
E_{LUMO} (eV)	-3.37	-3.38	-3.39	-3.39	-3.39
$ΔE_{HOMO-LUMO}$	3.37	3.36	3.35	3.35	3.35

168
169 **3.3 Solvation of particle transfer mechanism**
170
171 In this work, the gas-phase proton (H^+) and electron (e^-) enthalpies (H) used are respectively 6.197 and
172 3.145 kJ/mol [38]. The latter represents the integrated heat capacity at 298.15 K for ideal gas, $H(H^+)$ =
173 (5/2)RT, while the former is obtained from the Fermi-Dirac statistical mechanic equations. We used the
174 experimentally determined solvation enthalpies of the hydrogen atom $H(H^•)$ in benzene, methanol,

175   acetonitrile and water (**Table 3**). In gas phase, the average value of $\Delta_f H^\circ(H\bullet)$ (5 kJ/mol) obtained from [17]
176   was used. The solvation enthalpies of H^+ and e^- in various solvents have been computed at IEF-PCM/6-
177   311++G(d, p) level and the results obtained are in good agreement with experimental values. The
178   solvation enthalpies listed in **Table 3** have been computed as enthalpy changes of the following
179   processes [39]:

180     $$solvent_{(solv)} + H^+(g) \rightarrow solvent - H^+_{(solv)}$$ 14

181     $$solvent_{(solv)} + e^-(g) \rightarrow solvent^-_{(solv)}$$ 15

182   Our values of $\Delta_f H^\circ(H)$ and those reported in the literature calculat ed at the same level of theory are nearly
183   the same in all solvents used.

184   **Table 3. Solvation enthalpies of hydrogen atom ($\Delta_f H^\circ_{solv}(H^\bullet)$), proton ($\Delta_f H^\circ_{solv}(H+)$) and electron ($\Delta_f H^\circ_{solv}(e^-)$)**
185   **in kJ/mol**

Solvent	ε^a	$\Delta_f H^\circ_{solv}(H^\bullet)$	$\Delta_f H^\circ_{solv}(H+)$		$\Delta_f H^\circ_{solv}(e^-)$	
		a	This work	a	This work	a
Benzene	2.28	6.4	-878	-894	-14	-7
Methanol	32.7	5.0	-1016	-1038	-88.6	-86
Acetonitrile	35.69	5.0	-1060	-1031	-130	-95
Water	78.38	-4.0	-984.4	-1022	-131.2	-105

186   *a from Ref. [27]*

187   Presented in **Table 4** are the values (in kJ/mol) of BDE, IP, PA, PDE and ETE, parameters that describe
188   the mechanisms of antioxidant particle transfer.

189   **Table 4. Values of BDE, AIP, PDE, PA and ETE properties (in kJ/mol) in the studied mediums,**
190   **obtained by DFT/B3LYP/6-311++G(d,p)**

Medium	BDE	AIP	PDE	PA	ETE
Gas	371.52	738.15	910.20	1339.20	354.15
Benzene	372.48	679.30	754.30	1006.30	427.30
Methanol	370.45	536.40	639.97	757.92	418.40
Acetonitrile	370.45	529.00	639.81	755.81	413.00
Water	370.45	517.60	635.14	747.14	405.60

191
192   ### 3.3.1 Hydrogen atom transfer
193
194   The values of BDE for homolytic cleavage obtained by different mechanisms are presented in **Table 5**,
195   along with gas phase results found in the literature [8, 9]. In **table 5**, bond dissociation enthalpies
196   calculated by the HAT, SET-PT and SPLET mechanisms are represented by BDE, DBE_{e-p} and DBE_{p-e}
197   respectively. It is clear from this table that the gas phase BDE value obtained in this work is in very good
198   agreement with that obtained from literature [8, 9]. This table also shows that the BDE due to homolytic
199   fission is lower than DBE_{e-p} and DBE_{p-e} in all media. This led us to the conclusion that hydrogen atom
200   transfer by emodin occurs almost exclusively by the homolytic mechanism in all media. The effect of
201   solvation on the value of BDE is relatively insignificant since it has changed **approximately only by 1**
202   **kJ/mol from the gas** to the solvent phases. On the other hand, the values of DBE_{e-p} and DBE_{p-e} have
203   witnessed a reduction of about 540 kJ/mol, as media permittivity increases. This could be due to the fact

that AIP and PA, which are the rate determining properties of the two heterolytic mechanisms, are very
sensitive to solvation; as evidenced in table 4. Although the BDE_{p-e} and BDE_{e-p} values are identical, a
comparison of AIP and PA shows that the electron-proton sequential transfer has priority over the reverse
mechanism. It is equally obvious in this table that AIP and PA are each higher than the BDE in all media
investigated; which justifies the preference of the homolytic mechanism over heterolytic.

Table 5. Values of BDEs (in kJ/mol) in various media, obtained by B3LYP/6-311++G(d,p)

	BDE			BDE_{e-p}	BDE_{p-e}
	This work	[8]	[9]		
Gas	371.52	371.12	371.12	1693.34	1693.34
Benzene	372.48	_	_	1433.60	1433.60
Methanol	370.45	_	_	1176.37	1176.37
Acetonitrile	370.45	_	_	1168.81	1168.81
Water	370.45	_	_	1152.74	1152.74

3.3.2 Single electron transfer followed by proton transfer

Here, the main property studied is AIP. Our gas phase AIP value (783.15 kJ/mol) is in better agreement
with that obtained by [8] (775.81 kJ/mol), than that obtained by [9] (662.33 kJ/mol). Since these
researchers performed their calculations with G03, the differences between their AIP values and that
obtained in the present study are certainly due to different software versions. The trend in our AIP values
in the various media investigated is shown in **Fig. 2**.

From **Fig. 2**, it can be seen that the AIP values change considerably with media polarities. AIP decreases
as media permittivities increase. This parameter has dropped by a maximum of 220.55kJ/mol from the
gas phase to the aqueous solution, showing that solvation has an impact on the electron transfer
process. AIP values are found to be higher than ETE values. This can be explained by the fact that the
neutral form of emodin is more stable and consequently less reactive than its deprotonated form. The
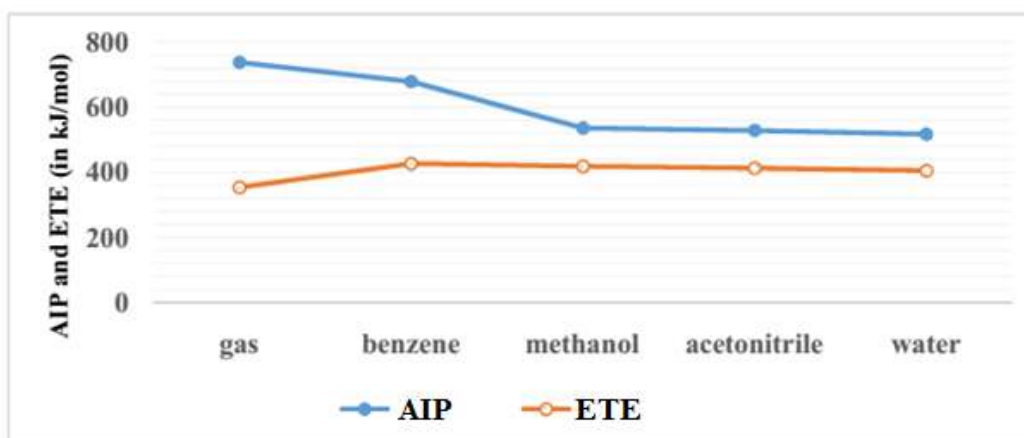ETE value is found to increase when solvation effects are considered.

225

226   ### 3.3.3 Sequential proton loss electron transfer

227

228   The main property that determines the rate of SPLET is PA. **Fig. 3** shows the variation of this property in
229   the various study media. It is obvious from the Fig. that PA decreases as solvent permittivity increases,
230   but remains fairly constant in the polar solvents. PA has reduced by a maximum of 592.06 kJ/mol from
231   the gas phase to the aqueous solution. The trend shown by BDE_{p-e} is similar to that shown by PA, since the
232   former is calculated using the latter. It is also noticed that the values of PA are relatively higher than those
233   of PDE. This is explainable based on the fact that the neutral form of emodin is more acidic than its
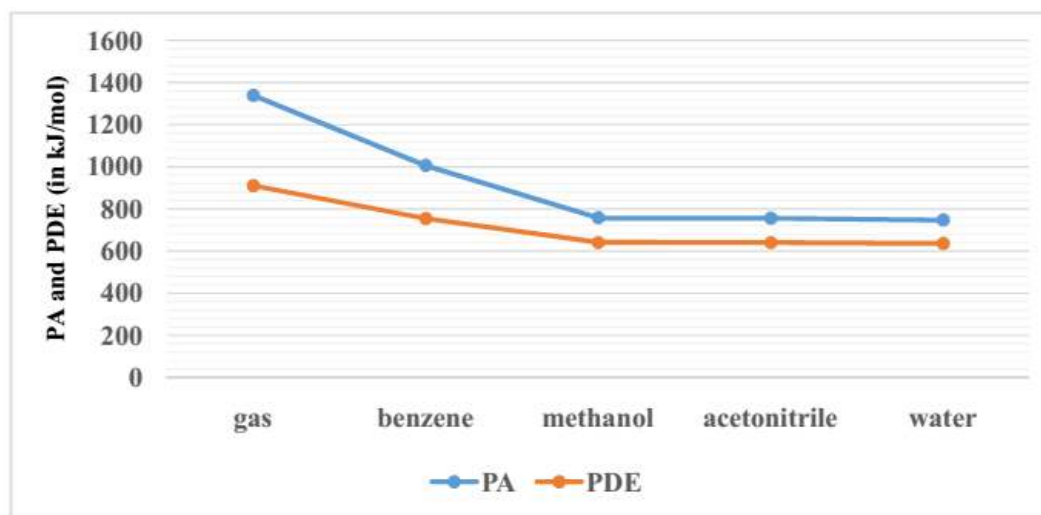234   ionized form.

236   **Fig. 3. Variation of PA and PDE of emodin in the different media, obtained by the DFT/B3LYP/6-**
237   **311++G(dp) method**

238

239   ## 3.4 Effects of solvation on the OH bond orbital occupation and charge

240

241   NBO analysis provides a deeper insight into atomic charge distribution, charge transfer and inter-orbital
242   interactions [36]. NBO parameters for the molecule studied are presented in **table 6**. From this table, it is
243   clear that the charge difference between oxygen and hydrogen, $|q_O| - |q_H|$ remains constant from gas phase
244   through the polar solvents. This can be attributed to the fact that both atoms of the free OH bond interact
245   with the molecules of each solvent leading to the formation of emodin-solvent hydrogen bonds. The
246   charge transferred from emodin's oxygen to the solvent's (methanol or water) hydrogen is replaced by
247   charge transferred from the solvent's oxygen to the substrate's acidic hydrogen. However, a reduction in
248   this charge difference is observed from gas phase to the nonpolar solvent (benzene). This reduction is
249   attributable to the fact that emodin-solvent charge transfer is made only from the emodin's oxygen to the
250   benzene hydrogens; the reverse transfer rendered impossible by the steric hindrance of the benzene ring.

251   The preceding observations are supported by the OH bond occupation in the different media investigated,
252   which increases from gas phase to benzene, but remains almost the same from gas phase to the polar
253   solvents.

254

255

Table 6. Values of atomic charge, charge differences and orbital occupancy of free OH bond in the investigated media

	Gas	Benzene	Methanol	Acetonitrile	water
Atoms	**Atomic charge** (in coulomb)				
O_2	-0.686	-0.683	-0.704	-0.704	-0.702
H_2	0.474	0.481	0.492	0.492	0.493
$\left\|q_O\right\| - \left\|q_H\right\|$	0.212	0.202	0.212	0.212	0.209
Bond	**Occupation, Q_{ij}**				
O_2-H_2	1.98556	1.98899	1.98561	1.98558	1.98536

3.5 Diffuse and polarized bases, and multiple division effect of valence atomic orbitals

The effects of diffuse and polarized bases, as well as multiple division effect of valence atomic orbitals have been studied only on BDE which characterizes the HAT mechanism for the antioxidant activity of emodin. This analysis has only been made on BDE because HAT is the most preferred antioxidant mechanism by emodin. The BDE values calculated with some Pople-typed basis sets along with their absolute relative values ($\left|\Delta BDE\right|$) obtained by comparison with the BDE value calculated with 6-311++G(d,p), are listed in **table 7**. Also present in this table, is the BDE value (371.52 kJ/mol) obtained by 6-311++G(d,p) in gas phase.

Clearly from **table 7**, the atomic orbital valence diffusion and their triple division do not practically affect the BDE value. In both cases, a BDE increment of less than 1 kJ/mol is observed. Indeed, the diffuse functions take account of a greater orbital occupation in a given area of space. These functions are essential in calculations involving transition metals and anionic systems; because the transition metal atoms have "d" orbitals which tend to be diffuse. The free electron of the anionic system could be far away from the rest of the electron density. However, the valence atomic orbital polarization especially those of hydrogen atoms, affect in a considerable manner, the energy of the O-H bond dissociation. The resulting variations are shown here to be higher than 10 kJ/mol and may reached 16.93 kJ/mol in the case of hydrogen atoms. It can be concluded that atomic orbital polarization, particularly, that of hydrogen atom is essential in determining the computational time for the X-H bond BDE. It is worth noting that these results are in agreement with the literature observations.

Table 7. BDE and $\left|\Delta BDE\right|$ values (in kJ/mol) of certain basis sets, relative to 6-311++G(d,p) in gas phase

	6-311++G**	6-311+G**	6-311G**	6-311++G*	6-311++G	6-311G	6-31++G**
BDE	371.52	372.39	371.78	354.59	360.99	359.51	371.17
$\left\|\Delta BDE\right\|$	0.00	0.87	0.26	16.93	10.53	12.01	0.35

4. CONCLUSION

Our results have revealed that solvation does not significantly affect the bond lengths and angles in emodin, but has a slightly appreciable impact on hydrogen bonds rendering them moderately strong. The stability of emodin from energetic studies increases slightly with solvent polarity. This result implies that the substrate-solvent interactions in this molecule are of Van der Waals type in non-polar solvents and of hydrogen bond type in polar solvents. The hydrogen atom homolytic transfer process has been identified as the dominating antioxidant mechanism of emodin in all media. The BDE value obtained in this work is in agreement with those obtained by [8, 9] in the gas phase. Our results have shown that diffusion and triple division of valence atomic orbitals do not influence the calculated BDE values in an appreciable manner, whereas they are significantly affected by polarization.

293

REFERENCES

295

[1] Urbaniak A, Molski M, Szelog M. Quantum-chemical calculations of the antioxidant properties of trans-p-coumaric acid and trans-sinapinic acid. Computation methods in Science and Technology. 2012;18(2):117-128.

[2] Amić A, Marković Z, Marković J M D, Stepanić V, Lučić B, Amić D. Towards an improved prediction of the free radical scavenging potency of flavonoids: The significance of double PCET mechanisms. Food Chemistry. 2014;152:578–585.

[3] Urbaniak A, Szela M, Molski M. Theoretical investigation of stereochemistry and solvent influence on antioxidant activity of ferulic acid. Computational and Theoretical Chemistry. 2013;1012:33–40.

[4] Valko M, Morris H, Cromiss M T D. Metals toxicity and oxidative stress. Current Medical Chemistry. 2005;12:1161-1208.

[5] Rahmawati I, Rejeki S E, Sardjiman. Antioxydant activity test of 2,6-bis(2'-furilidyn)-cyclohexanone: 2,5-bis-(2'-furilidyn)-cyclopentanone; 1,5-difuryl-1,4pentadien-3-one. Indonesia of cancer chemoprevention. 2010;1(1):38-43.

[6] Fifen J J, Nsangou M, Dhaouadi Z, Motapon O, Lahmar S. Single or double atom hydrogen transfer in the reaction of metal associated phenolic acids with OH° radical: DFT study. Journal of Molecular Structur: Theochem. 2009;901:49-57.

[7] Tamokou J d D, Chouna J R, Fischer-Fodor E, Chereches G, Barbos O, Damian G, Duma M, Nkeng-Efouet A P, Wabo K H, Kuiate J R, Mot A, Silaghi-Dumitrescu R. Anticancer and Antimicrobial Activities of Some Antioxidant-Rich Cameroonian Medicinal Plants. Journal pone. 2013;8:120-134.

[8] Jin R, Bao H. A DFT study on the radical scavenging activity of hydroxyanthraquinone derivatives in Rhubarb. Quantum Chemistry. 2010;111:1064-1071.

[9] Markovic′ S Z, Manojlovic T Z. DFT study on the reactivity of OH groups in emodin: structural and electronic features of emodin radicals. Monatsh Chemistry. 2009;140:1311–1318.

[10] Yen G C, Duh P D, Chuang D Y. Antioxidant activity of anthraquinones and anthrone. Food Chemistry. 2000;70:437-441.

[11] Aziz A N, Taha M, Ismail N H, Anouar E H, Yousuf S, Jamil W, Awang K, Ahmat N, Khan K M, Kashif S M. Synthesis, Crystal Structure, DFT Studies and Evaluation of the Antioxidant Activity of 3,4-Dimethoxybenzenamine Schiff Bases. Molecules. 2014;19:8414-8433.

[12] Hoelz L V B, Horta B A C, Araújo J Q, Albuquerque M G, de Alencastro R B, da Silva J F M. Quantitative structure-activity relationships of antioxidant phenolic compounds. J Chem Pharm Res. 2010;2(5):291-306.

[13] Anouar E, Calliste C A, Košinová P, Di Meo F, Duroux J L, Champavier Y, Marakchi K, Trouillas P. Free radical scavenging properties of guaiacol oligomers: a combined experimental and quantum study of the guaiacyl-moiety role. . Phys Chem A. 2009;113:13881–13891.

[14] Anouar E H, Raweh S, Bayach I, Taha M, Baharudin M S, Meo F D, Hasan M H, Adam A, Ismail N H, Weber J F F, Trouillas P. Antioxidant properties of phenolic Schiff bases: structure–activity relationship and mechanism of action. J Comput Aided Mol Des. 2013;27:951-964.

[15] Anouar E H, Shah S A A, Hassan N B, Moussaoui N E, Ahmad R, Zulkefeli M, Weber J F F. Antioxidant Activity of Hispidin Oligomers from Medicinal Fungi: A DFT Study. Molecules. 2014;19:3489-3507.

[16] Frisch M J, Trucks G W, Schlegel H B, Scuseria G E, Robb M A, Cheeseman J R, Scalmani G, Barone V, Mennucci B, Petersson G A, Nakatsuji H, Caricato M, Hratchian H P, Izmaylov A F, Bloino J, Zheng G, Sonnenberg J L, Hada M, Ehara M, Toyota K, Fukuda R, Hasegawa J, Ishida M, Nakajima T, Honda Y, Kitao O, Nakai H, Vreven T, Montgomery J A, Peralta J E, Ogliaro F, Bearpark M, Heyd J J, Brothers E, Kudin K N, Staroverov V N, Kobayashi R, Normand J, Raghavachari K, Rendell A, Burant J C, Iyengar S S, Tomasi J, Cossi M, Rega N, Millam J M, Klene M, Knox J E, Cross J B, Bakken V, Adamo C, Jaramillo J, Gomperts R, Stratmann R E, Yazyev O, Austin A J, Cammi R, Pomelli C, Ochterski J W, Martin R L, Morokuma K, Zakrzewski V G, Voth G A, Salvador P, Dannenberg J J, Dapprich S, Daniels A D, Farkas O, Foresman J B, Ortiz J V, Cioslowski J, Fox D J. 2009. Gaussian 09, Revision A.02. Gaussian, Inc, Wallingford CT.

349 [17] Fifen J J, Nsangou M, Dhaouadi Z, Matapon O, Jaidane N. Solvent effets on the antioxidant
350   activity of 3,4-dihydroxyphenylpyruvic acid : DFT and TD-DFT studies. Journal of Molecular
351   Structure: Theochem. 2011;966:232-243.
352 [18] Pople J A. Theoretical Models for Chemistry. Journal of Computational Chemistry. 2004;25:1925-
353   2004.
354 [19] Xue Y, Zheng Y, An L, Dou Y, Liu Y. Density functional theory study of the structure–antioxidant
355   activity of polyphenolic deoxybenzoins. Food Chemistry. 2014;151:198–206.
356 [20] Marković Z, Đorović J, Dekić M, Radulović M, Marković S, Ilić M. DFT study of free radical
357   scavenging activity of erodiol. Chemical Papers. 2013;67(11):1453–1461.
358 [21] Leopoldini M, Rondinelli F, Russo N, Toscano M. Pyranoanthocyanins: A Theoretical
359   Investigation on Their Antioxidant Activity. J Agric Food Chem. 2010;58:8862–8871.
360 [22] Mikulski D, Górniak R, Molski M. A theoretical study of the structure–radical scavenging activity
361   of trans-resveratrol analogues and cis-resveratrol in gas phase and water environment. European
362   Journal of Medicinal Chemistry. 2010;45:1015–1027.
363 [23] Mikulski D, Szela M, Molski M and Górniak R, Quantum-chemical study on the antioxidation
364   mechanisms oftrans-resveratrolreactions with free radicals in the gas phase, water and ethanol
365   environment, Journal of Molecular Structure: THEOCHEM 951, 2010, 37–48.
366 [24] Mikulski D, Molski M. Quantitative structure–antioxidant activity relationship oftrans-resveratrol
367   oligomers,trans-4,4'-dihydroxystilbene dimer,trans-resveratrol-3-O-glucuronide, glucosides:Trans-
368   piceid,cis-piceid,trans-astringin and trans-resveratrol-4'-O-β-D-glucopyranoside. European
369   Journal of Medicinal Chemistry. 2010;45:2366–2380.
370 [25] Bentes A L A, Borges R S, Monteiro W R, de Macedo L G M, Alves C N. Structure of
371   Dihydrochalcones and Related Derivatives and Their Scavenging and Antioxidant Activity against
372   Oxygen and Nitrogen Radical Species. Molecules. 2011;16:1749-1760.
373 [26] Najafi M. On the antioxidant activity of the orthoand metasubstituted daidzein derivatives in the
374   gas phase and solvent environment. J Mex Chem Soc. 2014;58(1):36-45.
375 [27] Nikolic K M. Theoretical study of phenolic antioxidants properties in reaction with oxygen-
376   centered radicals. Journal of Molecular Structure: THEOCHEM. 2006;774:95–105.
377 [28] Urbaniak A, Molski M, Szeląg M. Quantum-chemical Calculations of the Antioxidant Properties of
378   trans-p-coumaric Acid and trans-sinapinic Acid. Computational methods in science and
379   technology. 2012;18(2):1-12.
380 [29] Trouillas P, Marsal P, Svobodová A, Vostálová J A, Gažák K, Hrbáč J, Sedmera P, Křen V,
381   Lazzaroni R, Duroux J-K, Walterova D. Mechanism of the antioxidant action of silybin and 2,3-
382   dehydrosilybin flavonolignans: a joint experimental and theoretical study. J Phys Chem A.
383   2008;112:1054-1063.
384 [30] Nikolic K M. Theoretical study of phenolic antioxidants properties in reaction with oxygen-
385   centered radicals. Journal of molecular structure: THEOCHEM. 2006;774:95–105.
386 [31] Wang G, Xue Y, An L, Zheng Y, Dou Y, Zhang L, Liu Y. Theoretical study on the structural and
387   antioxidant properties of some recently synthesised 2,4,5-trimethoxy chalcones. Food Chemistry.
388   2015;171:89–97.
389 [32] Chen Y, Xiao H, Zheng J, Guizhao L. Structure-thermodynamics-antioxidant activity relationships
390   of selected natural phenolic acids and derivatives: an experimental and theoretical evaluation.
391   PLoS ONE. 2015;10(3):1-20.
392 [33] Cao H, Cheng W-X, Li C, Pan X-L, Xie X-G, Li T H. DFT study on the antioxidant activity of
393   rosmarinic acid. Journal of Molecular Structure: THEOCHEM. 2005;719:177–183.
394 [34] Jeremić S, Filipović N, Peulić A, Marković Z. Thermodynamical aspect of radical scavenging
395   activity of alizarin and alizarin red S. Theoretical comparative study. Computational and
396   Theoretical Chemistry. 2014;1047:15–21.
397 [35] Steiner T. The Hydrogen Bond in the Solid State. Angew Chem Int Ed. 2002;41:48-76.
398 [36] Mohamed M E. Structure-antioxidant activity relationship study of eugenol derivatives using semi-
399   empirical method. New York Science Journal. 2013;6(1):102-106.
400 [37] Bruns R E, Haiduke R L A, Do-Amaral A T. The Linear Relationship Between Koopmans' and
401   Hydrogen Bond Energies for some Simple Carbonyl Molecules. J Braz Chem Soc.
402   2002;13(6):800-805.

403 [38] Najafi M, Farmanzadeh D, Klein E, Zahedi M. A theoretical study on the enthalpies of homolytic
404 and heterolytic N–H bond cleavage in substituted melatonins in the gas–phase and aqueous
405 solution. Acta Chim Slov. 2013;60:43–55.
406 **[39]** Nono J H, Bikélé M D, Ghogomu N J, Younang E, Mbaze M L L, Lissouck D, Zobo M J, Shridhar
407 R G. DFT-Study on Antioxydant of 3-alkyl-4-phenylacetylamino-1H-1,2,4-triazol-5-ones and its
408 derivatives, J Chem Chem Eng, 2014;8:43–55.